Available online at www.sciencedirect.com

ScienceDirect

Procedia Structural Integrity 8 (2018) 43–55

Structural Integrity Procedia

www.elsevier.com/locate/procedia

AIAS 2017 International Conference on Stress Analysis, AIAS 2017, 6-9 September 2017, Pisa, Italy

Analytical Stiffness Matrix for Curved Metal Wires

E. Marotta[a], P. Salvini[a*]

[a]*Department of Enterprise Engineering, University of Rome "Tor Vergata", via del Politecnico, 1 00133 - Rome - ITALY*

Abstract

The paper presents an analytic stiffness matrix for curved thin metal wires, derived by the application of the second Castigliano's Theorem. The matrix accounts both bending and axial stiffness contributions in plane. The beam geometry is described by a cubic polynomial function of the curvature radius with a monotonical attitude angle as the independent variable. The solution proposed if fully analytical although a consistent number of adding factors appear. Some test cases are discussed and compared with Finite Element solutions, formed by a plentiful assembly of straight beams.

Peer-review under responsibility of the Scientific Committee of AIAS 2017 International Conference on Stress Analysis

Keywords: Stiffness Matrix; Curved Beam, Metal Wires; Net Structures; Cubic Interpolation

1. Introduction

Deployable Space Antennas present some peculiar needs that require clever solutions for the engineers to overcome. First of all weight minimization and packing inside the space rocket before the deployment in the space. Reflectors are as large as 12 m (Thomson, 2000), but much more higher diameters are at present time in the design stage. The mechanism involved in the deployment phase includes the use of very light nets, usually made of molybdenum or tungsten wires, knitted to form the mesh. The knitting procedure is very critical (Marotta et al., 2016) since wires as small as 15 microns are used. It is straightforward to get a mechanical characterization of the net to verify that the

* Corresponding author. Tel.: +39.06.7259.7140; Fax +39.06.7259.7145
E-mail address: salvini@uniroma2.it

Peer-review under responsibility of the Scientific Committee of AIAS 2017 International Conference on Stress Analysis
10.1016/j.prostr.2017.12.007

antenna presents a stable behaviour against solar irradiation changes, which strongly influence the satellite performances. The mechanical characterization has been carried out by measuring the behaviour of a portion of the net on a two-dimensional testing machine (Valentini et al., 2016), properly developed to accurately measure very low loads when large displacements are imposed. Difficulties arise because the wires slide each other during deformation, so that traditional systems for measuring strains are not easily applicable. In De Salvador et al. (2017) an optical device to measure strains is discussed.

As a result of the knitting procedure, and having in mind the strength of tungsten wires, the net results as a regular repetition of loops with a high ratio between voids and wires. In the present paper we introduce the idea to model the wires of the net considering their repetitive pattern and their non-linear behaviour. The base element is thus a very thin wire in comparison with the loop diameter. In other words, we need to develop a solution for general curved beams in plane, subjected to axial and bending loads. The final goal here is to develop a finite element with two extremal nodes, able to match the stiffness of a beam with variable curvature.

Many structures of engineering interest are suitably modelled with curved beams. One of the most practical methods to analyse and design such structures is the finite element method. The calculation is often undertaken by modelling the curved structure with a series of short straight beams and the solution, of course, is approximate (Kikuchi, 1975). Increasing the number of elements arises the accuracy, but the dimension of the problem also rises. The mechanical behaviour of a curved beam can be expressed through the equations of equilibrium, constitutive relationships and compatibility equations or by mean the equations of energy (Tabarrok et. al., 1988); in any case, the solution requires numerical integration. As a matter of fact, the analytical solutions proposed are limited to trivial shapes of the axis-line of the curved beam, such as circular or parabolic shapes (Marquis e Wang, 1989). In most cases a numerical integration technique is unavoidable, so that a real closed form solution is missing.

The Castigliano's Theorem is particularly suitable to obtain the flexibility matrix, and consequently the stiffness matrix of the generic beam. This method requires the computation of the strain energy, which is then differentiated by respect to a selected force. Repeating the differentiation for each displacement in turn, a complete set of force-displacement equations is achieved, the whole results can then be formulated in a matrix notation (Przemieniecki, 1968). Stiffness matrix formulation for constant curved beam are presented by Lee, (1969) and Palaninathan and Chandrasekharan (1985), flexural, axial and shear effects are taken into account. One numerical application of this method is proposed by Dayyania, et. al. (2014), to obtain a general super element for a curved beam applicable to corrugated panels. The effect of the thick curved beam element with constant curvature was considered by Litewka and Rakowski (1998). Marquis e Wang (1989) have developed an exact solution of a parabolic curved beam with constant cross section considering bending, axial extension and shear deformation effects. Using a modified Hu-Washizu variational principle, Saje (1991) derived a finite element formulation of deformation analysis of arbitrarily curved, extensible, shear flexible beam. Koziey and Mirza (1994) have formulated a consistent subparametric beam element. They applied cubic and quadratic polynomial approximations for displacements and rotation, respectively, using elements described in the natural coordinate system.

The greatest difficulty to extract the stiffness matrix is the solution of the energy integral of the beam. Many authors have proposed several approaches to overcome this issue. Some authors, such as Leung and Au (1990), attempted to exploit the spatial description through spline curves. While Lin et al. (2009) proposed a closed form solution of the circular, spiral ellipse, parabola, cycloid, catenary and logarithmic spiral beam under pure bending moment. Farouki (1996) presents an advanced spline interpolation such as Pythagorean-hodograph curves, described in the field of complex numbers, which solved the rational integrals in energy calculation. Wu and Yang (2016) proposed a method to obtain an interpolation of curvature radius for given G1 or G2 boundary data, with or without prescribed arc lengths, by solving a linear system. The radius function has a low order polynomial with a monotone angle as the independent variable.

Gimena et al. (2014) present a general differential formulation for the case of the arch. In the paper, they did not make use of energetic theorems involving derivatives. They developed two examples of arcs with parabolic axis-line and variable cross-section, subjected to concentrated or distributed load.

Tufekci and Arpaci (2006) discussed an exact analytical solution for in-plane static problems of planar curved beams with variable curvatures and variable cross-sections. The solutions, non-general for any arch shape, are derived by using the initial value method. The fundamental matrix required by the initial value method is obtained analytically. Then, displacements, slopes and stress resultants are found analytically along the beam axis by using the fundamental matrix. The method was then extended to the case of distributed load structures from Tufekci et al. (2016).

The nonlinear extension introduced by Rafik and El Damatty (2002) is based on a total Lagrangian approach. The

derivation of the nonlinear stiffness matrix and the unbalanced load vector is presented. Newton-Raphson method is employed for iterating purpose and the energy method is used as convergence criterion.
In the work here proposed, a two-dimensional formulation in the closed form of the stiffness matrix is presented, for a curved beam subjected to pure bending. The axial contribution must be considered to gain the solution stability.
The curvature radius of the wire is modelled by a polynomial law; whose independent variable is the local angle of alignment. The solution assumes that the angle must necessarily vary monotonically.
Polynomial law coefficients are calculated by interpolation. The adoption of a cubic polynomial allows expressing several families of curves, thus providing the model for many applications.
The stiffness matrix derives by inversion of the flexibility matrix whose analytical terms are directly calculated using the Castigliano's method. The resulting integrals to solve are composed of many simple recursive functions.
The stiffness matrix obtained is very well suited for modelling structures both in the field of small displacements and for large displacements, since incremental calculations are easily possible. Numerical comparisons are performed to validate the stiffness matrix obtained, from a multi-element modelling that uses multiple straight-beams.
Due to wire applications, there is no need to account of shear effects or to foresee any change in the sections of the beams. Furthermore, distributed loads are not taken into account.
Fig. 1 shows a portion of a typical astromesh reflector; as it can be seen, the wire diameter is small compared to the loop extensions.

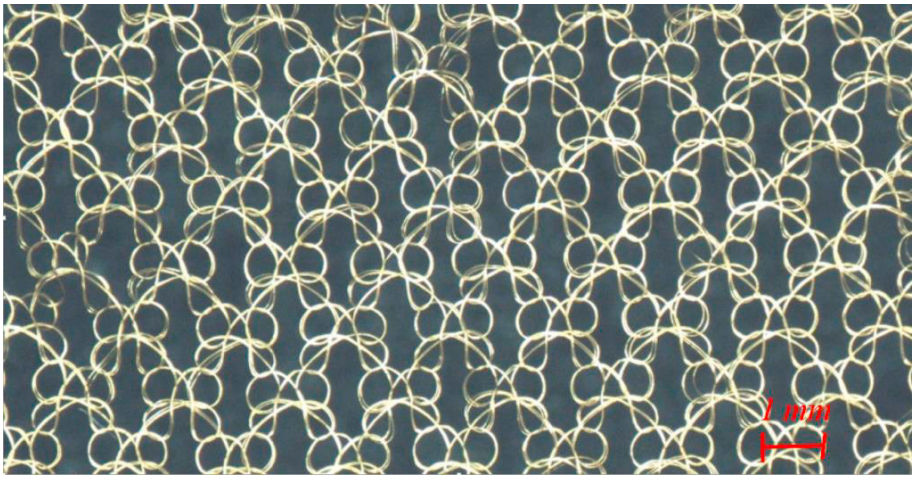

Fig. 1. A portion of typical astromesh reflector.

2. Derivation of Stiffness Matrix

In this approach, limited to plane domain, the stiffness matrix is derived by the (3x3) inversion of the analytical solution of the flexibility matrix in two different constrain conditions. Each term of the flexibility matrix is computed through the application of the Second Castigliano's Theorem. According to it, the displacement and rotational vectors can be obtained from partial derivation of the total strain energy. In the foregoing procedure the internal energy due to bending behaviour and tension-compression are computed separately. This need comes out from the lengthy of the expressions involved in the analytical developments. Considering the internal bending energy:

$$\delta_i = \frac{\partial U}{\partial P_i} = \frac{\partial}{\partial P_i}\int \frac{M^2(s)}{2EI} ds = \int \left[\frac{M(s)}{EI}\right]\left[\frac{\partial M(s)}{\partial P_i}\right] ds \tag{1}$$

Where δ_i is the generalized displacement component, U is the bending energy, P_i the load applied and oriented as the displacement considered, M is the bending occurring at the curvilinear abscissa s, E is the Young's modulus, I is the section inertia moment. In the case hereinafter considered, that the cross-section keeps constant, eq.1 becomes:

$$\delta_i = \frac{1}{EI}\int M(s)\left[\frac{\partial M(s)}{\partial P_i}\right]ds \tag{2}$$

The expression of *ds*, in the Cartesian reference, results

$$ds = \sqrt{dx^2 + dy^2} \tag{3}$$

This term introduces complexity in the analytical integration. An idea to circumvent these difficulties emerges by the change of variable, from the curvilinear abscissa to the angle given by the local tangent of the beam. This substitution yields

$$ds = \rho(\theta)\,d\theta \tag{4}$$

where $\rho(\theta)$ is the radius of curvature and $d\theta$ is the elementary variation of attitude. This change of variable implicates that the new variable θ increases or decreases monotonically, for analytical integration needs.
With the aim to include a generality of curved beams, but keeping the analytical integration possible, the choice fells on a polynomial expression, limited to the cubic interpolation of the curvature radius

$$\rho(\theta) = a\cdot\theta^3 + b\cdot\theta^2 + c\cdot\theta + d \tag{5}$$

Thanks to this substitution, the Cartesian coordinates follow by simple integration of product of a polynomial and cosine (or sine) functions

$$x(\varphi) = \int_0^{\varphi} \rho(\theta)\cdot\cos\theta\, d\theta \tag{6}$$

$$y(\varphi) = \int_0^{\varphi} \rho(\theta)\cdot\sin\theta\, d\theta \tag{7}$$

The solution of the above integrals, at a generic angle θ, are

$$\begin{aligned} x(\theta) = {} & a\sin\theta\cdot\theta^3 + b\sin\theta\cdot\theta^2 + 3a\cos\theta\cdot\theta^2 - 6a\sin\theta\cdot\theta + c\sin\theta\cdot\theta + 2b\cos\theta\cdot\theta - 2b\sin\theta + \\ & + d\sin\theta - 6a\cos\theta + c\cos\theta + 6a - c \end{aligned} \tag{8}$$

$$\begin{aligned} y(\theta) = {} & -a\cos\theta\cdot\theta^3 + 3a\sin\theta\cdot\theta^2 - b\cos\theta\cdot\theta^2 + 2b\sin\theta\cdot\theta + 6a\cos\theta\cdot\theta - c\cos\theta\cdot\theta - 6a\sin\theta + \\ & + c\sin\theta + 2b\cos\theta - d\cos\theta - 2b + d \end{aligned} \tag{9}$$

The knowledge of the Cartesian coordinates of the curve is crucial to carry out the bending moment acting along the curvilinear beam. Fig. 2 is an example of a curve that is manageable with the polynomial approach in the local coordinate system. It is clear that no matter if closed loops are considered.

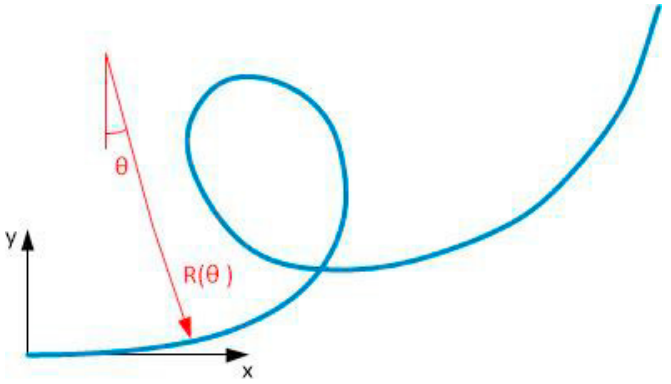

Fig. 2. A generic curve and its local coordinate system.

The cubic interpolation of the radius curvature allows simplifying the solution of the integrals; but the inference from the curved geometry and its description, in terms of these said coefficients, needs to be explicated. The developed solution implies three circumstances:

- The local x-axis must be set so that it is oriented as the initial beam tangent
- Tangent angle is monotonically varying so that the curvature function never changes the sign within the considered domain of integration
- Infinity radius, representing straight geometry, cannot be managed and should be considered as straight lines

In a general curvilinear beam, the appropriate coefficients of the polynomial representation rise by interpolation of the actual curve. Ordinary Least Square methods fit well. In fact eq.s (8) and (9) allows to write a linear system of equations where the known terms are some curve coordinates at specific θ angles. It is very useful to add to those equations a further information, written in eq. (10), concerning the total length of the wire; adding a considerable weight to this equation addresses the solution towards the effective shape.

$$L(\theta)=\frac{1}{4}a\theta^4+\frac{1}{3}b\theta^3+\frac{1}{2}c\theta^2+d\theta \tag{10}$$

Fig. 3 shows the isostatic scheme used to carry out the flexibility terms of the curved wire at the first end. Node 1 has three degree of freedom and node 2 is fully constrained.

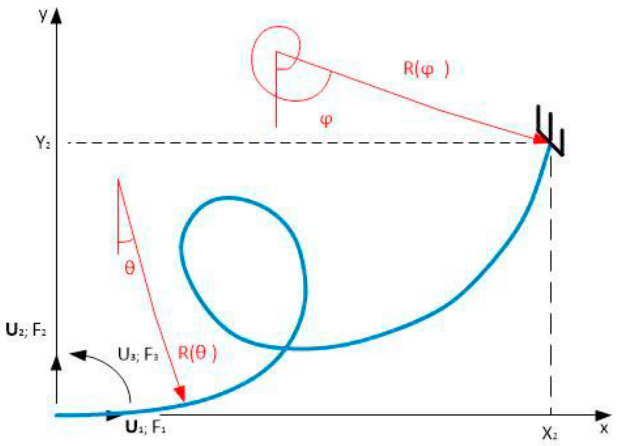

Fig. 3. First isostatic scheme.

Pointing attention, as an example, to the displacement u_1 due to an applied load F_1, the solution arises from the integral

$$u_1 = \frac{1}{EI}\int_0^{\varphi} M(\theta)\cdot\frac{\partial M(\theta)}{\partial F_1}\cdot\rho(\theta)d\theta \tag{11}$$

The first compliance term c_{11} thus requires to compute the bending moment as a function of θ

$$\begin{aligned} M(\theta) = F_1\cdot y(\theta) = F_1\cdot(&-a\cos\vartheta\cdot\vartheta^3 + 3a\sin\vartheta\cdot\vartheta^2 - b\cos\vartheta\cdot\vartheta^2 + 2b\sin\vartheta\cdot\vartheta + 6a\cos\vartheta\cdot\vartheta + \\ &- c\cos\vartheta\cdot\vartheta - 6a\sin\vartheta + c\sin\vartheta + 2b\cos\vartheta - d\cos\vartheta - 2b + d) \end{aligned} \tag{12}$$

The integral (11) results composed by the product of several terms

$$c_{11} = \frac{1}{EI}\int_0^{\varphi}\left(\begin{matrix}-a\cos\vartheta\cdot\vartheta^3 + 3a\sin\vartheta\cdot\vartheta^2 - b\cos\vartheta\cdot\vartheta^2 + 2b\sin\vartheta\cdot\vartheta + 6a\cos\vartheta\cdot\vartheta + \\ -c\cos\vartheta\cdot\vartheta - 6a\sin\vartheta + c\sin\vartheta + 2b\cos\vartheta - d\cos\vartheta - 2b + d\end{matrix}\right)^2\cdot\left(a\cdot\theta^3 + b\cdot\theta^2 + c\cdot\theta + d\right)d\theta \tag{13}$$

The resulting integral is very long, but, after the application of double-angle formulae, it results as composed by sine and cosine recursive integral terms, such those given by eq.(14) and eq.(15).

$$\int x^n\sin(cx)dx = -\frac{x^n}{c}\cos(cx) + \frac{n}{c}\int x^{n-1}\cos(cx)dx \tag{14}$$

$$\int x^n\cos(cx)dx = -\frac{x^n\sin cx}{c} - \frac{n}{c}\int x^{n-1}\sin(cx)dx \tag{15}$$

Indeed, an enormous number of trivial terms occurs, all of them supply an analytical solution, but easily manageable using a symbolic solver.
Repeating eq.11 for all the three degrees of freedom of the beam, it is possible to obtain, in closed form, the matrix of flexibility of the first structure shown in Figure 3.

$${}^1\left|\begin{Bmatrix}u_1\\u_2\\u_3\end{Bmatrix} = \begin{bmatrix}c_{11} & c_{12} & c_{13}\\ c_{21} & c_{22} & c_{23}\\ c_{31} & c_{32} & c_{33}\end{bmatrix}\cdot\begin{Bmatrix}F_1\\F_2\\F_3\end{Bmatrix}\right. \tag{16}$$

The inversion of the flexibility matrix provides the constrained stiffness matrix in the reference of node 1

$${}^1\mathbf{K}_{II} = \begin{bmatrix}c_{11} & c_{12} & c_{12}\\ c_{21} & c_{22} & c_{23}\\ c_{31} & c_{32} & c_{33}\end{bmatrix}^{-1} = \begin{bmatrix}k_{11} & k_{12} & k_{12}\\ k_{21} & k_{22} & k_{23}\\ k_{31} & k_{32} & k_{33}\end{bmatrix} \tag{17}$$

To obtain the second part of the stiffness matrix it is necessary to constrain the node 1 and apply loads at node 2.

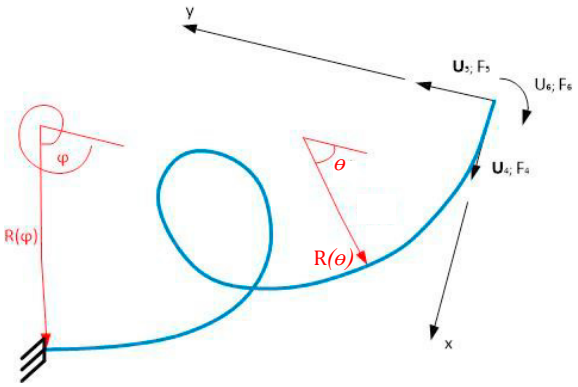

Fig. 4. Second isostatic scheme.

The same equation as before is valid, as long as a different reference system, on node 2, is now considered (Fig. 4)

$$\rho'(\theta) = a \cdot (\varphi - \theta)^3 + b \cdot (\varphi - \theta)^2 + c \cdot (\varphi - \theta) + d \tag{18}$$

The new coefficients, identified by an apex, can be related to the previous computed ones if the spanning angle is given by $\varphi - \theta$, after equating the curvature radius given by eq.s (5) and (18). The new coefficients result

$$\begin{aligned} a' &= -a \\ b' &= b + 3a\varphi \\ c' &= -3a\varphi^2 - 2b\varphi - c \\ d' &= a\varphi^3 + b\varphi^2 + c\varphi + d \end{aligned} \tag{19}$$

The nomenclature for the flexibility matrix links the forces at node 2 with the displacements at the same node

$$^2\left| \begin{Bmatrix} u_4 \\ u_5 \\ u_6 \end{Bmatrix} = \begin{bmatrix} c_{44} & c_{45} & c_{46} \\ c_{54} & c_{55} & c_{56} \\ c_{64} & c_{65} & c_{66} \end{bmatrix} \cdot \begin{Bmatrix} F_4 \\ F_5 \\ F_6 \end{Bmatrix} \right. \tag{20}$$

accordingly, the constrained stiffness matrix is:

$$^2\mathbf{K}_{jj} = \begin{bmatrix} c_{44} & c_{45} & c_{46} \\ c_{54} & c_{55} & c_{56} \\ c_{64} & c_{65} & c_{66} \end{bmatrix}^{-1} \tag{21}$$

Now the $^2K_{jj}$ matrix refers to the second local coordinate system. This second stiffness matrix is reconducted to the first reference by the simple rotation

$$^1\mathbf{K}_{JJ} = \mathbf{T}_{21}^T \cdot {}^2\mathbf{K}_{JJ} \cdot \mathbf{T}_{21} \tag{22}$$

Where the transformation matrix, note sign opposite to usual, is given by

$$\mathbf{T}_{12}=\begin{bmatrix}-\cos\varphi & -\sin\varphi & 0\\ -\sin\varphi & \cos\varphi & 0\\ 0 & 0 & -1\end{bmatrix} \tag{23}$$

To complete the 6x6 stiffness matrix, which relates the forces at node 1 to the displacements at node 2, equilibrium conditions are invoked

$$^{1}\left|\begin{Bmatrix}F_4\\F_5\\F_6\end{Bmatrix}=\begin{bmatrix}-1 & 0 & 0\\ 0 & -1 & 0\\ -(Y_2-Y_1) & (X_2-X_1) & -1\end{bmatrix}\begin{Bmatrix}F_1\\F_2\\F_3\end{Bmatrix}=[\mathbf{G}]\cdot\begin{Bmatrix}F_1\\F_2\\F_3\end{Bmatrix}=[\mathbf{G}]\cdot[\mathbf{K}_{II}]\begin{Bmatrix}u_1\\u_2\\u_3\end{Bmatrix}=[\mathbf{K}_{JI}]\begin{Bmatrix}u_1\\u_2\\u_3\end{Bmatrix}\right. \tag{24}$$

Where X_1, Y_1, X_2, Y_2, are the node coordinates respectively of node 1 and 2. All values are expressed in the reference located at node 1.
The stiffness matrix in the same reference system emerges by composition of the previous partial matrices.

$$^{1}\mathbf{K}=\begin{bmatrix}\mathbf{K}_{II} & \mathbf{K}^{T}_{JI}\\ \mathbf{K}_{JI} & \mathbf{K}_{JJ}\end{bmatrix} \tag{25}$$

Bending stiffness is not sufficient to gives stability to the matrices, when the section loads result oriented as the local tangent. Therefore, the axial contribution is computed again by Castigliano's theorem.

$$u_i=\frac{1}{EI}\int_0^{\varphi}P(\theta)\cdot\frac{\partial P(\theta)}{\partial F_i}\cdot\rho(\theta)d\theta \tag{27}$$

The axial stiffness contribution acts in series with the bending stiffness, therefore its contribution is simply added at the flexibility matrix, derived from pure bending treatment.

$$^{1}\left|\begin{Bmatrix}u_1\\u_2\\u_3\end{Bmatrix}=\begin{bmatrix}c_{11}+a_{11} & c_{12}+a_{12} & c_{13}\\ c_{21}+a_{21} & c_{22}+a_{22} & c_{23}\\ c_{31} & c_{32} & c_{33}\end{bmatrix}\cdot\begin{Bmatrix}F_1\\F_2\\F_3\end{Bmatrix}\right. \tag{28}$$

$$^{2}\left|\begin{Bmatrix}u_4\\u_5\\u_6\end{Bmatrix}=\begin{bmatrix}c_{44}+a_{44} & c_{45}+a_{45} & c_{46}\\ c_{54}+a_{54} & c_{55}+a_{55} & c_{56}\\ c_{64} & c_{65} & c_{66}\end{bmatrix}\cdot\begin{Bmatrix}F_4\\F_5\\F_6\end{Bmatrix}\right. \tag{29}$$

Applying eq.s (16-25) allows to get the matrix of the bending-axial curved.

3. Test Cases

The first interesting point is to highlight the family of curved functions that can be fitted by the approximated strategy provided here. To accomplish this task, a simple set of curves are represented in Fig. 5, all of them characterized by the same ending points.

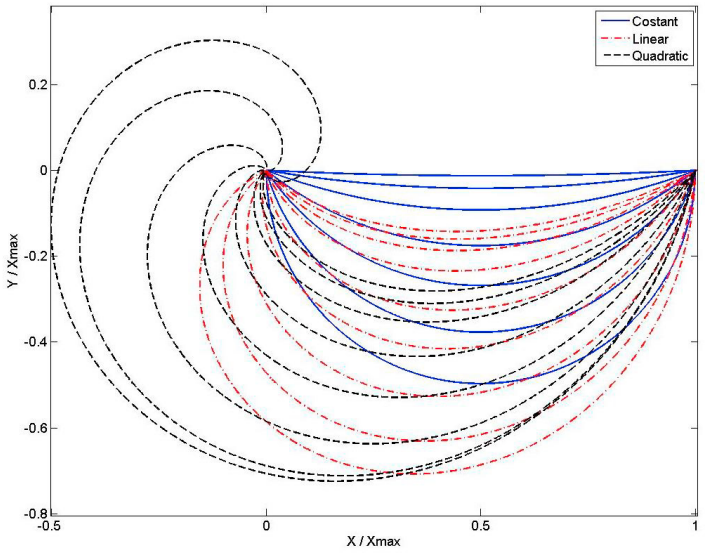

Fig. 5. Family of possible curves as power of the tangent angle.

The family of curves are grouped in this way: continuous or blue line have constant curvature radius; dash-dot or red lines have linear-varying radius; dash-dash lines have quadratic radius of curvature, cubic variations are not represented to make it easy the analysis of the picture at a glance. The geometric lines that are manageable comes from a combination of these basic types. Whenever the attention is pointed on a curved wire that does not present a monotonical increase of the tangent angle, it can be subdivided in several parts respecting this last requirement. An effective example is presented in Fig. 6, taken from a knitted astromesh reflector. The coloured segments identify the basic structure that form the entire mesh, when repeated at neighbour patterns after mirroring or flipping. In synthesis, four coloured sequence form a repeated pattern. The different colours (blue, red, green, cyan) distinguish the regions where monotonical θ increase holds; other reasons for the requirement of element division comes out for an unacceptable fitting (e.g. splitting of blue and red parts).

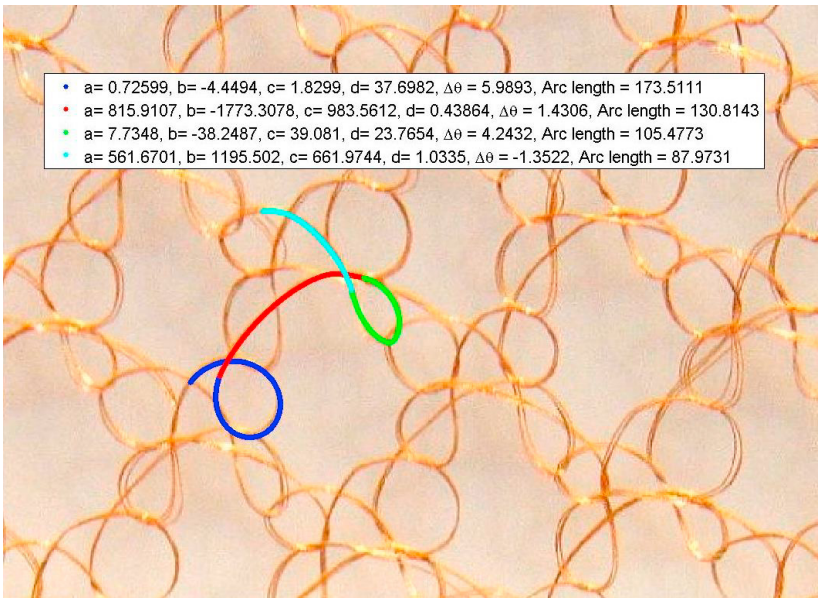

Fig. 6. A portion of astromesh and its modelling by four curved beam element, coefficients are within the picture.

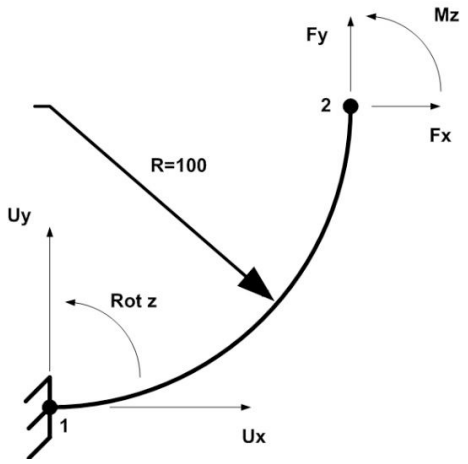

Fig. 7. Scheme of a cantilever circular beam.

Test cases deal with a single element configuration having 3 different geometries and load dispositions. Each curved wire, modelled with appropriate coefficients, is compared with a multi-beam fem model, consisting of 1000 small straight elements. All test cases refer to a local reference system pointed on first node 1.
First test case consists of a quarter circle with constant radius. The circular wire is steel made and has a diameter as 1 mm, curvature radius 100 mm, and 206 GPa Young's modulus. The node 1 is fully constrained and the forces are applied on node 2. The displacement comparisons by the analytical curved beam and Finite Element results are presented in Table 1. For this simple test case, a simple theoretical solution is also available to compare. The analytical displacements are perfectly corresponding to the expected theoretical values. FEM results are slowly scattered because they suffer the number of elements used. Decreasing the numbers of straight beam elements causes the error to increase, as expected.

Table 1. Displacements of cantilever circular beam, for curved beam model, multi-beams and theoretical value

Force at Node 1 [N]		Displacement [mm]	Curved Beam (1 element)	Multi Beam (1000 elements) No Shear Effect	Theoretical
Fx =	0.01	Ux	0.77670388	0.77670283	0.77670388
		Uy	-0.49445887	-0.49445847	-0.49445887
		Rot z	-0.00988924	-0.00988923	-0.00988924
Fy =	0.01	Ux	-0.49445887	-0.49445847	-0.49445887
		Uy	0.35225411	0.35225399	0.35225411
		Rot z	0.00564474	0.00564474	0.00564474
Mz =	1	Ux	-0.98892392	-0.98892267	-0.98892392
		Uy	0.56447414	0.56447376	0.56447414
		Rot z	0.01553398	0.01553397	0.01553398

A second test is sketched in Fig. 8. The curved beam has now a linearly growing radius, cross section and material are the same as before. The scheme between the two nodes is now different, resulting a simply-supported beam. The only load applied is a concentrated moment at node 1, rotations on both ending nodes are picked up. The results are shown in Table 2. The comparison is again almost perfect by respect to FEM, but no theoretical well known values are simply available.

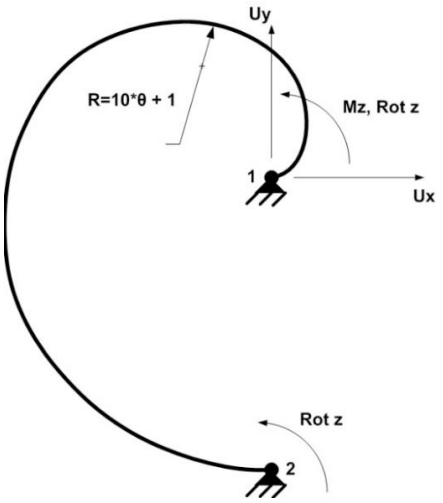

Fig. 8 .Spiral beam geometry.

Table 2. Displacements of spiral beam comparison with multi-beam model.

Force at Node 2 [N]		Displacement [mm]	Curved Beam (1 element)	Multi Beam (1000 elements) No Shear Effect	Err [%]
Mz =	10	Rot z (Node 1)	0.12450012	0.12449944	0.000550464
		Rot z (Node 2)	0.05564610	0.05564565	0.000822931

In the last test, a most general case with cubic polynomial representation of the radius is presented, so that all four coefficients are not vanishing. The curved beam is fully constrained on node 1 and loads are applied on node 2. The results are displayed in Table 3. Again, for this more general case, errors between the analytical developed curved beam and the multi-beam FE model are very low.

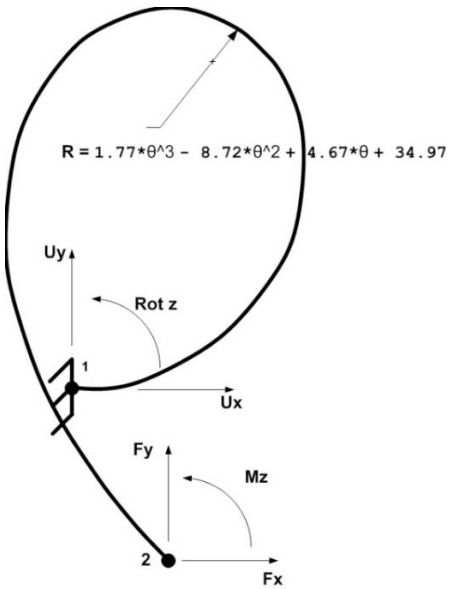

Fig. 9. Generic curved beam geometry.

Table 3. Displacements of generic curved beam comparison with a multi-beam FE model.

Force at Node 1 [N]		Displacement [mm]	Curved Beam (1 element)	Multi Beam (1000 elements) No Shear Effect	Err [%]
Fx =	0.01	Ux	0.45762659	0.45762582	0.000168236
		Uy	0.02259979	0.02259967	0.000554164
		Rot z	0.00811160	0.00811159	0.000116319
Fy =	0.01	Ux	0.02259979	0.02259967	0.000554165
		Uy	0.04198039	0.04197990	0.001165151
		Rot z	0.00077002	0.00077001	0.000945798
Mz =	1	Ux	0.81116035	0.81115941	0.000116319
		Uy	0.07700169	0.07700096	0.000945797
		Rot z	0.01806017	0.01806014	0.000190059

It appears evident, in all tests, the convenience to use this analytical curved beam element at the place of the assembled multi beams. According to the said refinement and in plain domain, the number of dof's in the stiffness matrix reduces from 6006 to 6. This means that a knitted net can be appropriately modelled keeping it reasonable the overall number of dof's.

4. Conclusion

In the present work, a closed solution for the stiffness matrix of curved beam is proposed. The planned solution makes use of the second Castigliano's Theorem. Both bending and axial effects are taken into account. The analytical solution is carried out for a curved beam through a cubic function of the radius of curvature. This interpolation allows to manage analytically all integrals, since it yields terms that can be resolved by recursive application of integrals of simple functions. The coefficients of the cubic function are given by Least Square interpolation; however, if interpolation results non-satisfactory, the wire can be divided in portions, each appropriately fitted. The displacement comparisons with multi-beam fem models demonstrate the truthfulness of the solution. As a matter of fact, no approximations are introduced within the frame of Euler Beam theory.

The present work allows to model structures made of curved wires, such as the metal nets for space applications, by means of very few elements, in the contest of an exact solution.

The method is also very promising for nonlinear analyses, when high displacements and eventual mutual contacts are considered. At each step the interpolating coefficients can be recomputed in the new equilibrium position. Further researches are now under investigation, and will be the subject of successive works.

References

Dayyania, I., Friswell, M. I., Saavedra Flores, E. I., 2014. A general super element for a curved beam. International Journal of Solids and Structures vol. 51, 2931–2939.

De Salvador, W., Marotta, E., Salvini, P., 2017. Strain Measurements on Compliant Knitted Mesh Used in Space Antennas, by means of 2D Fourier Analysis. Accept for publication on Strain.

Farouki. R.T., 1996. The elastic bending energy of Pythagorean-hodograph curves. Computer Aided Geometric Design 13, 227-241.

Gimena, F.N., Gonzaga, P., Gimena, L., 2014. Analytical formulation and solution of arches defined in global coordinates. Engineering Structures, Vol. 60, 189–198

Kikuchi, F., 1975. On the validity of the finite element analysis of circular arches represented by an assemblage of beam elements. Computer Methods in Applied Mechanics and Engineering, No. 5, 253-276.

Koziey, B.L., Mirza, F.A.,1994. Consistent curved beam element. Computers & Structures 51 No. 6, 643–654.

Lee, H.P., 1969. Generalized stiffness matrix for a curved beam element. AIAA J. 7, 2043-2045.
Leung, A.Y.T., Au, F.T.K.,1990. Spline finite elements for beam and plate. Computers & Structures 37 No. 5, 717-729.
Lin, K.C., Lin, C.W., Lin, M.H., 2009. Finite deformation of 2D curved beams with variable curvatures. Journal of Solid Mechanics and Materials Engineeting, vol.3, No. 6, 876-886.
Litewka P, Rakowski J.,1998. The exact thick arch finite element. Computers and Structures, vol.68, 369-379.
Marotta, E., De Salvador W., Pennestrì E., Salvini P., Scialino, L., Valentini, P.P., 2016. Some problems arising during the experimental characterization of compliant knitted mesh. 37th Esa Antenna workshop, Esa/Estec, 15-17 November 2016
Marquis, J.P., Wang, T.M., 1989. Stiffness matrix of parabolic beam element. Computers & Structures Vol 31 No. 6, 863-870.
Palaninathan, R., Chandrasekharan, P.S., 1985. Curved beam element stiffness matrix formulation. Computers & Structures Vol 21 No.4, 663-669.
Przemieniecki, J.S., 1968. Theory of matrix structural analysis. McGraw-Hill, New York.
Rafik R. G., El Damatty, A. A., 2002 Large displacement analisys of curved beams. 4th Strutural Specialty Conference of the Canadian Society for Civil Engineering
Saje, M., 1991. Finite element formulation of finite planar deformation of curved elastic beams. Computers & Structures Vol 39 No. 3/4, 327–337
Tabarrok, B., Farshad, Yi, H., 1988 . Finite element formulation of spatially curved and twisted rods. Computer Methods in Applied Mechanics and Engineering, N. 70, 275-299.
Thomson, M.W., 2000. The astromesh deployable reflector, Iutam-Iass Symposium on Deployable structures: Theory and Applications, 80, 435–446.
Tufekci E, Arpacı A., 2006. Analytical solutions of in-plane static problems for non-uniform curved beams including axial and shear deformations. Struct Eng Mech 22(2), 131–150.
Tufekci E., Ugurcan E., Serhan A., 2016. A new two-noded curved beam finite element formulation based on exact solution. Engineering With Computers .· August 2016
Valentini,P.P., Falcone, M., Marotta, E., Pennestrì, E., Salvini, P.,2016. Theoretical and experimental characterization of a FEM element assembly for the simulation of very compliant knitted mesh . International Journal for Numerical Method in Engineering, Vol. 107, 419–429.
Wu, W., Yang, X., 2016. Geometric Hermite interpolation by a family of intrinsically defined planar curves. Computer-Aided Design 77, 86–97.